Depth-Graded Multilayers for Linear Zone-Plate Applications

Chian Liu [a)], R. Conley, A. T. Macrander, and J. Maser
Experimental Facilities Division, Argonne National Laboratory, Argonne, IL 60439

H. C. Kang, M. A. Zurbuchen, and G. B. Stephenson
Material Science Division, Argonne National Laboratory, Argonne, IL 60439

Fresnel zone plates for x-ray focusing optics are typically made using lithographic techniques. To achieve optimum efficiency for hard x-rays, a depth of several microns is required, which limits the minimum zone width and hence minimum focal spot size achievable using lithography. We are exploring the fabrication of zone plates by an alternative technique that surmounts these limitations: the growth of a multilayer film in which the thickness of consecutive layers gradually increases according to the Fresnel zone formula; the film is subsequently sectioned to the required depth. For a planar multilayer, this produces a linear zone plate that can focus x-rays in one dimension. Here we report the growth and characterization of a depth-graded multilayer suitable for use as a zone plate for hard x-ray focusing. The multilayer has a total of 470 alternating layers of WSi_2 and Si with thicknesses increasing monotonically from 15 to 60 nm, for a total thickness of 11.33 μm. One of the major challenges is to understand and select the right material system for this kind of thick multilayers. We have found that WSi_2/Si is a promising system. A comparison between WSi_2/Si and W/Si multilayers is presented.

I. INTRODUCTION

Modern synchrotron radiation facilities provide unprecedented levels of brilliant and highly collimated x-ray beams and offer tremendous research opportunities. Development of improved x-ray focusing optics is essential for further advances in x-ray microimaging and microanalysis applications. Focusing optics for x-rays differ from those for visible light, as the refractive index of solids is slightly smaller than unity for x-rays and significantly greater than unity for visible light. Reflective x-ray mirrors, such as elliptical Kirkpatrick-Baez (KB) mirrors and tapered hollow capillaries,[1-3] can be used only at very small grazing angles below the critical angle of the reflecting material. Refractive lenses for x-rays have the opposite curvature to that for visible light. A solid focusing lens for visible light corresponds to a cavity with the same shape for x-rays. Since the refractive index is very close to one, a series of concave lenses is needed to give a reasonable focal length for x-rays. This kind of refractive lenses, using low-absorbing materials, has been used to focus x-rays.[4] While submicron x-ray spots have been achieved with reflective and refractive optics, the smallest x-ray focal spots obtained were produced using Fresnel zone plates. Spatial resolution on the order of 20 nm in the soft x-ray range has be reported.[5,6]

Fresnel zone-plate lenses are diffractive optics. Traditional zone plates are circular transmission gratings consisting of alternating transparent and opaque (or phase-shifting) rings. Each ring (or zone) is positioned so that the optical path from the zone plate to the primary focus differs by $\lambda/2$ between consecutive zones, where λ is the x-ray wavelength. X-rays diffracted by the zones thus add “in phase” at the primary focus. The optimum zone positions are given by the Fresnel zone-plate formula [7-9]

$$r_n^2 = n\lambda f + n^2\lambda^2/4, \qquad (1)$$

where r_n is the radius of the nth zone, and f is the focal length. The second term in Eq. (1) is a correction for spherical aberration and can be omitted when $n\lambda << f$. The width of the nth zone is $(r_n - r_{n-1})$. The focusing capability of a zone plate depends on the width of the outermost zone, the optical contrast between the alternating zones, and the accuracy of the zone placement. For optimized x-ray zone-plate materials, depths of several microns are typically required for efficient focusing of hard x-rays.

Traditional zone plates are fabricated using lithographic techniques. To achieve the required high aspect ratio of zone depth to width, a mask with the zone-plate pattern is first made using e-beam lithography, and x-ray lithography is then used with a thick resist and subsequent metal electroplating on silicon nitride membranes for zone-plate fabrication.[10] Tremendous progress has been made in this field, and very recently a spatial resolution of 60 nm was achieved for hard x-rays using zone plates with a 50 nm outermost zone width and 1 μm zone depth with gold as the zone material.[11, 12] However, as the desired zone width becomes smaller and zone depth larger, the manufacturing process becomes increasingly difficult.

An alternative approach to the fabrication of hard x-ray zone plates is the deposition and sectioning of multilayers. The techniques for producing x-ray multilayers have advanced tremendously over the past 35 yrs.[13-15] The thickness of deposited films can be controlled in the angstrom range, much more precisely than the x-y positioning in a lithographic system. With slicing and polishing, large aspect ratios can easily be obtained. To date, sectioned, multilayer-coated wires have been used for zone plates.[16, 17] In this process, a rotating thin, round wire is sputter-coated with a multilayer structure, where the position of each layer follows the zone-plate formula. In this case, the first layer coated is the thickest and nearest to the optical axis. A 0.2 μm focal spot has been achieved at an x-ray energy of 12.4 keV using 50 zones with an outermost zone width of 0.1 μm coated on gold wires of ~50 μm diameter.[17] There are several factors limiting the achievable resolution with this technique. First, the wires are not ideally round or smooth at the nanoscale, affecting the uniformity of zone positions. Second, with the outermost zone coated last, it is very difficult to achieve the desired accuracy of zone placement. Third, when coating on a round wire, there is unavoidably oblique incidence of the sputter atoms, causing a shadowing effect and leading to film roughness.[18] Apparently, achieving focal spots much smaller than 0.2 μm using sputtered-sliced wires is very difficult.

We have recently been exploring the fabrication of linear zone plates using sputtered-sliced multilayers grown on flat Si substrates.[19-21] As illustrated in Fig. 1, two identical planar multilayer sections would be assembled to form the two halves of a linear zone plate, to produce a focus in one dimension. The separation of the two halves allows them to be tilted at the optimum angle for high diffraction efficiency. Another pair rotated by 90° about the optical axis could be used to produce a point focus. Since the multilayer sections are assembled with the substrate side oriented away from the optical axis, the thinnest zones can be grown first, minimizing the impact of accumulated growth imperfections on zone-plate performance. There are three major challenges to growing the linear zone-plate multilayer structures. First, it is necessary to find a multilayer system having both low stress and good adhesion to survive the subsequent cutting and polishing. Second, an understanding of the growth process of the multilayer is needed so that each zone layer can be precisely placed. Third, a computer program to automatically perform the prolonged deposition according to the zone-plate formula and the growth-rate correction for each layer must be set up. In this paper, we present our solutions to these challenges.

II. STUDIES OF W/Si AND WSi_2/Si MULTILAYER GROWTH

We have investigated two multilayer systems: WSi_2/Si and W/Si on Si substrates. All depositions reported here were carried out at the Advanced Photon Source deposition lab using dc magnetron sputtering, which has been previously described.[22] The substrates were loaded on a carrier with the optical surface facing down and were alternately translated back and forth over two 3-in.-diameter planar sputter guns during deposition. The substrate-to-target distance was 107 mm with no bias applied to the substrates. Laterally uniform depositions were achieved through the design of shaped apertures above the sputter guns.[23] The sputter guns were operated at a constant current of 0.5 A, and the film thicknesses were controlled by the translation speeds and the number of loops over the gun according to growth-rate calibrations. The guns were programmed to turn on 7 sec before the substrate was moved over and to turn off after a desired thickness was deposited. This procedure reduces the use of the target material, lowers the target temperature, and helps ensure comparable growth conditions for each sequential layer growth.

To satisfy the zone-position requirement of Eq. (1), the thickness of each layer must be precisely controlled. We need to understand the growth rate for each multilayer component and how the growth rate changes during the growth of each layer and over the course of the multilayer deposition. For these purposes, periodic multilayer test samples were grown using different procedures and measured using x-ray reflectance. Analysis of the reflectivity was done with the aid of IMD, a computer program for modeling the optical properties of multilayers.[24,25] Reflectivity measurements were made in θ–2θ geometry over the range from $0 < \theta < 6^{\circ}$, using Cu-Kα_1 x-rays with a collimating multilayer optic followed by a Ge crystal monochromator. The measured data were compared with that calculated using the IMD software for a best fit to determine layer thicknesses and interface parameters.

The following procedure was designed to understand the multilayer growth and to calibrate the growth rates. Two $12.5 \times 25 \times 0.5$ mm^3 Si test substrates (cut from an ordinary wafer) were loaded on the substrate holder ~40 cm apart. Two different [WSi_2/Si] $\times$ 15 multilayers were grown on these substrates with certain fixed moving speeds when they were passing the sputter guns. For substrate A, three loops over the WSi_2 gun and two loops over the Si gun were used to complete a bilayer. For substrate B, two loops over the WSi_2 gun and three loops over the Si gun were used to complete a bilayer. The fitted thickness for Si was 50.28 Å for sample A and 75.42 Å for sample B, and for WSi_2 was 36.12 Å for A and 24.08 Å for B. The results indicate that the thicknesses of both WSi_2 and Si scale linearly with the number of loops over the target. The same procedure was later used to study W/Si multilayers, with W replacing WSi_2 and with different fixed speeds. This time the Si thickness was 20.58 Å for sample A and 37.85 Å for sample B, and the W thickness was 52.92 Å for A and 35.65 Å for B. The thicknesses for W and Si do not scale linearly with the number of loops. In other words, the traditional scaling method using the deposition time for thickness control cannot be applied to the W/Si multilayer system but can be used in the WSi_2/Si system. One possible explanation is that Si is very reactive with W, and a portion of the deposited Si and incoming Si atoms might have diffused into W for the W/Si multilayer system during deposition and cannot be accounted for in the simulation, as reported in the literature. [26] For the WSi_2/Si system, this effect is negligible, since WSi_2 is already a silicide. We will come back to this issue later.

We have measured stoichiometry of a sputtered WSi_2 film using energy dispersive x-ray (EDX) analyses. The average ratio of Si to W was 1.874±0.118.

The desired total thickness of the multilayer for the zone-plate application is quite large, at least a few microns for each multilayer material. The growth rate may change from the beginning to the end of deposition. How the rate changes with the target use has to be measured and incorporated in the calculation of the growth of each zone layer. To demonstrate the change of the growth rate with the target use, three Si targets with different target erosion levels were selected for three sets of WSi_2/Si × 15 and W/Si × 15 multilayers under identical growth conditions and the same substrate translation speeds. Only the number of loops over the Si gun was changed: one for sample A, two for B, and three for C. A total of 18 samples were grown and measured with x-rays and analyzed with the IMD software. Three $12.5 \times 25 \times 0.5$ mm^3 Si substrates were loaded at one time, ~40 cm apart, for one set of multilayer growth. Figure 2 summarizes the results of the Si layer thickness as a function of Si deposition time. The WSi_2 (and W) layer thicknesses were very close in value for each set of samples. The three Si targets are: "new" – barely used, "middle" – with a erosion depth of ~4.8 mm, and "old" – with a erosion depth of ~6.1 mm. The targets were all 3 inches in diameter and 0.25 inch in thickness. From Fig.

2, one can see that the growth rate decreases with target use, with the decrease most rapid when the target is new. We thus use only targets that have been moderately used for zone-plate multilayer growth. Also one can clearly see that the Si layer thickness does not extrapolate to zero at zero growth time for W/Si, in contrast to the case for WSi_2/Si. The nonlinearity of layer thicknesses with deposition time has been previously reported for the W/Si multilayer system using x-ray reflectance analyses and IMD software. [26] Interfacial diffusion, mixing due to energetic bombardment, and resputtering were attributed as possible causes for the nonlinearity. Our studies support the case for interdiffusion, since the WSi_2/Si system obeys a linear scaling. It is well known that multilayers consisting of chemically reacting materials (such as W/Si and Mo/Si) suffer more diffusive mixing and are less stable than multilayers consisting of nonreacting materials (such as WSi_2/Si and $MoSi_2$/Si). [27, 28] The diffusive mixing in these multilayers is a dominant factor in interfacial imperfection. In our pursuit of small-d-spacing multilayers for narrow-bandpass monochromator applications, we have found that WSi_2/Si multilayers have sharper interfaces than W/Si multilayers. [29] Because of its linear growth rate behavior and sharp interfaces, WSi_2/Si is an ideal multilayer system for linear zone-plate applications. An added advantage for the WSi_2/Si system is the relatively high growth rate. Under the same growth conditions, Si grows ~8 times faster than other traditional low-Z materials such as C or B_4C. A high growth rate is critical for thick zone-plate growth.

By using periodic multilayer and x-ray analysis, one can thus determine the initial growth rate and drift of the growth rate with the growth time for the WSi_2/Si system. In addition to the target-erosion effect, drift of the growth rate may also be related to a linear decline of the sputter gun voltage at the constant-current mode observed in Si and WSi_2 depositions. Later experiments confirmed a slower drift of the growth rate when a constant-power mode was used for sputter power supplies. In the following, we discuss how to grow a linear zone-plate multilayer structure.

III. THE GROWTH OF LINEAR ZONE-PLATE MULTILAYERS

A linear zone-plate structure is also defined by Eq. (1), with r_n defined as the distance between the outer edge of the nth zone and the optical axis. One may choose an outermost zone width and calculate the zone-plate structure according to the intended x-ray energy range and focal length. For our test sample, we have chosen an outermost zone of 15 nm, λ = 0.413 Å (30 keV), and f = 10.89 mm. One may use the same zone plate at different energies by adjusting the focal length. For fixed λ and f, the maximum number of zones is determined by the width of outermost zone, Δr_{out}, according to:

$$n_{\max} \approx f\lambda/4(\Delta r_{\text{out}})^2. \tag{2}$$

Equation (2) is easily derived from Eq. (1) by taking a derivative of r_n and using the condition of $\lambda \ll f$. From Eq. (2), we have $n_{\max}$ of 500 for our test zone plate with $r_{500} \approx$ 15 µm. Then from Eq. (1) and (r_n - $r_{n\text{-}1}$), the layer thickness of each zone was obtained. Zone 500 with a width of ($r_{500} - r_{499}$) ≈ 15 nm is the outermost zone (Layer 1). It is not necessary to fabricate the full zone structure to produce a focusing optic; the diffraction-limited resolution of a partial zone-plate structure simply varies inversely with the size of the partial structure. We chose to fabricate the zone structure from zone 31 to zone 500, for a total of 470 layers and a total deposition thickness of r_{500} - r_{30} = 11.33 µm. Zone 31 has a width of ($r_{31} - r_{30}$) ≈ 60 nm and is the last-coated layer (Layer 470).

When the outermost zone is thin, the difference between neighboring outer zones becomes very small. In our test zone-plate structure, the thickness difference between the first and second WSi_2 layer (Zone 500 and Zone 498) is only 0.3 Å. To produce an ideal zone plate, the layer positions in the structure must be controlled to within a small fraction of the layer width. This means that the accumulated thickness error over hundreds of layers totaling ~10 μm thickness should be less than a few nanometers. The resolution of the substrate speed control should therefore be significantly smaller than 1×10^{-4} so that it does not contribute significantly to the accumulated error. The transport in our deposition system is driven by a microstepping motor with built-in indexing, manufactured by Compumotor.[30] The indexer can resolve velocities to the 5^{th} decimal place, while the speed we use is in the first decimal place. Growth-rate tests were used to determine the initial speeds for a 1 nm deposition per loop for each material. The required thickness for each zone layer in units of nm determines how many loops to use, and the remainder is distributed equally into each loop with a calculated difference in speed. A computer program was developed to calculate the thickness of each layer from Eq. (1) and the time needed for its growth, taking into account the decrease in growth rate during multilayer deposition. A linear decrease of growth rate of 7.5% over the whole deposition duration was used for the growth correction for the WSi_2/Si multilayer, apportioned according to the accumulated "target on" time. This computer program compiles a command script to be executed by the system control program.

Using this control system, the zone-plate multilayer structure was grown in 2.3 mTorr argon onto five $12.5 \times 25 \times 0.5$ mm^3 Si substrates. The coating was carried out automatically and took ~32 h to finish for the WSi_2/Si system. The same zone-plate multilayer structure was also grown using W/Si with a total growth time of ~45 h. We noticed that the targets used in growing the W/Si multilayer were "older", which might contribute to the longer growth time also. The W/Si zone-plate multilayer cracked and peeled from the substrate on the edges of the multilayer. WSi_2/Si multilayers with the same thickness and multilayer structure remained intact and survived subsequent slicing and polishing.

IV. CHARACTERIZATION OF THE WSi_2/Si LINEAR-ZONE PLATE MULTILAYER

The face of the WSi_2/Si zone plate multilayer was glued to another Si substrate and sectioned to ~1 × 2 mm^2 pieces using a diamond dicing saw. Figure 3 shows a scanning electron microscope (SEM) image of the polished cross section of the multilayer. The bright strips are WSi_2, and the dark ones are Si. The image shows flat and sharp interfaces of the multilayer. A gradual increase in d-spacing from ~30 nm to 120 nm is clearly seen. The thinnest bright strip on the left is Zone 500 (Layer 1), and the dark strip on the right is Zone 31 (Layer 470). A noticeably thinner Si strip, identified as Zone 81 (Layer 420), is visible at ~79% of the total multilayer thickness on the image. A fallen flake from the detachment of the Si deposit on the shield can might have caused a temporary short of the Si gun during the growth of that layer. We noticed quite a few fallen flakes on the bottom of the Si deposition chamber. For WSi_2, the situation was much better; WSi_2 has a better adhesion to the inner walls of the shield can. The Si gun was off center at the time, with one side closer to the wall of the can. Since then we have modified the deposition chamber so that the gun is centered in the shield can. Also, the inside of the shield can, especially the upper part directly facing the gun, was roughened to increase the adhesion. We noticed improved stability of the sputter guns afterwards.

The SEM images of the multilayer cross section were analyzed to determine the positions of every layer in the multilayer. Comparison of images from different regions gave consistent results within a few nanometers. Figure 4 compares the measured layer positions from SEM with the targeted layer positions (r_{500} - r_n) from Eq. 1. The measured positions deviate increasingly from the targeted values as the layer number increases. This is presumably due to an overcorrection of the decrease in growth rate. Further accumulation and analysis of the growth-rate change with deposition thicknesses are needed for a more accurate growth control. Figure 5 shows the inverse of the layer spacing $1/\Delta r_n$ versus layer position r_n. According to Eq. (1), this plot should be a straight line (for $\lambda << f$) with a slope equal to $-2/\lambda f$. Although the measured values do not have the same slope as the target values, for the first 8 μm of the structure they do follow a reasonably straight line. A fit to this region gives a focal length of f = 10.27 mm at λ = 0.0413 nm compared to the designed value of f = 10.89 mm at λ = 0.0413 nm.

Thin cross sections of the multilayer were obtained by polishing a sawn section on both faces to the desired section depth. The focusing properties of a section having a depth of 19 μm were measured at beamline 12-BM of the Advanced Photon Source, at an x-ray energy of 19.5 keV (λ = 0.0636 nm). The incident beam only illuminated the 8 μm region of the multilayer structure having layer positions following the zone-plate formula. A focal spot size ~72 nm was measured.[31] This compares well to the diffraction-limited focal spot size of 68 nm that would be obtained from an ideal partial zone plate of this size and outermost zone width.

V. SUMMARY

We have demonstrated the feasibility of using planar depth-graded multilayers in fabricating high-aspect-ratio linear zone plates for hard x-ray focusing applications. We found that WSi_2/Si is a promising candidate for growing such multilayers with the required layer-position accuracy. Detailed studies of uniform W/Si and WSi_2/Si multilayers demonstrated that WSi_2/Si multilayers have more predictable growth rates and sharper interfaces than W/Si ones. WSi_2/Si multilayers with layer spacings following the Fresnel zone-plate formula for an outermost zone width of 15 nm have been successfully grown. Analysis of SEM images showed deviations from the targeted layer positions but verified that an acceptable zone-plate structure was obtained over the first 8 μm of the deposition, which produced nearly diffraction-limited focusing performance.

ACKNOWLEDGMENTS

We thank M. Kirk and R. Koritala for help of EDX analyses and R. Khachatryan and G. Czop for technical assistance, all from Argonne National Laboratory. This work is supported by the U. S. Department of Energy, Office of Science, Office of Basic Energy Sciences, under Contract No. W-31-109-ENG-38.

REFERENCES

[a] Electronic mail: cliu@aps.anl.gov

1. P. Kirkpatrick and V. Baez, J. Opt. Soc. Am. **38**, 766 (1948).
2. C. Liu, R. Conley, L. Assoufid, Z. Cai, J. Qian, and A. T. Macrander, AIP Conf. Proc. **705**, 704 (2004).
3. D. H. Bilderback, S. A. Hoffman, and D. J. Thiel, Science **263**, 201 (1994).
4. B. Lengeler, C. G. Schroer, M. Richwin, J. Tummler, M. Drakopoulos, A. Snigirev, and I. Snigireva, Appl. Phys. Lett. **74**, 3924 (1999).
5. M. Peuker, App. Phys. Lett. **78**, 2208 (2001).
6. W. Chao, E. Anderson, G. P. Denbeaux, B. Harteneck, J. A. Liddle, D. L. Olynick, A. L. Pearson, F. Salmassi, C. Y. Sony, and D. T. Attwood, Opt. Lett. **28**, 2019 (2003).
7. J. Kirz, J. Opt. Soc. Am. **64**, 301 (1974).
8. E. Spiller, *Soft X-ray Optics*, SPIE Optical Engineering Press, Bellingham, WA, 1994.
9. J. Als-Nielsen and D. McMorrow, *Elements of Modern X-ray Physics*, John Wiley & Sons, New York, 2001.
10. A. A. Krasnoperova, J. Xiao, F. Cerrina, E. Di Fabrizio, L. Luciani, M. Figioment, M. Gentill, W. Yun, B. Lai, and E. Gluskin, J. Vac. Sci. Technol. B **11**, 2588 (1993).
11. U. Neuhausler and G. Schneider, AIP Conf. Proc. **705**, 1255 (2004).
12. W. Yun, private communication (2004). www.xradia.com.
13. T.W. Barbee, Opt. Eng. **25**, 898 (1986).
14. B. L. Henke, E. M. Gullikson, J. Kerner, A. L. Oren, and R. L. Blake, J. X-ray Sci. Technol. **2**, 17 (1990).
15. T. Salditt, D. Lott, T. H. Metzger, J. Peisl, G. Vignaud, P. Hoghoj, O. Scharf, P. Hinze, and R. Lauer, Phys. Rev. **54**, 5860 (1996).

16. R. M. Bionta, E. Ables, O. Clamp, O. D. Edwards, P. C. Gabriele, K. Miller, L. L. Ott, K. M. Skulina, R. Tilley, and T. Viada, Opt. Eng. **29**, 576 (1990).

17. N. Kamijo, Y. Suzuki, M. Awaji, A. Takeuchi, H. Takano, T. Ninomiya, S. Tamura, and M. Yasumoto, J. Synchrotron Rad. **9**, 182 (2003).

18. J. A. Thornton, J. Vac. Sci. Technol. A **4**, 3059 (1988).

19. H. C. Kang, G. B. Stephenson, C. Liu, R. Conley, A. T. Macrander, J. Maser, S. Bajt, and H. N. Chapman, Proc. SPIE **5537**, 127 (2004).

20. J. Maser, G. B. Stephenson, S. Vogt, W. Yun, A. T. Macrander, H. C. Kang, C. Liu, and R. Conley, Proc. SPIE **5539**, 194 (2004).

21. H. C. Kang, G. B. Stephenson, C. Liu, R. Conley, A. T. Macrander, J. Maser, S. Bajt, and H. N. Chapman, Appl. Phys. Lett. **86**, 151109 (2005).

22. C. Liu, J. Erdmann, J. Maj, and A. T. Macrander, J. Vac. Sci. Technol. A **17**, 2741 (1999).

23. C. Liu, R. Conley, L. Assoufid, A. T. Macrander, G. E. Ice, T. Z. Tischler, and K. Zhang, J. Vac. Sci. Technol. A **21**, 1579-1584, 2003.

24. D. L. Windt, Computers in Physics, **12**, 360 (1998).

25. D. L. Windt 2004, http://cletus.phys.columbia.edu/~windt/idl/.

26. D. L. Windt, F. E. Christensen, W. W. Craig, C. Hailey, F. A. Harrison, M. Jimenez-Garate, R. Kalyanaraman, and P. H. Mao, J. Appl. Phys. **88**,460 (2000).

27. A. I. Fedorenko et al., Proc. SPIE **2453**, 11 (1995).

28. A. I. Fedorenko et al., Proc. SPIE **2453**, 15 (1995).

29. C. Liu, R. Conley, A. T. Macrander, T. Graber, Ch. Morawe, C. Borel, and E. M. Dufresne, Proc. SPIE **5537**, 154, 2004.

30. Compumotor Division, Parker Hannifin Corp., Rohnert Park, CA 94928.

31. H. C. Kang, M. A. Zurbuchen, G. B. Stephenson, C. Liu, R. Conley, A. T. Macrander, J. Maser, unpublished (2004).

FIGURE CAPTIONS

Fig. 1 Schematic cross sections through: a) a standard zone plate fabricated by lithography; b) a zone plate fabricated by deposition and sectioning of depth-graded multilayers.

Fig. 2 Si layer thickness as a function of growth time for 6 sets of WSi_2/Si (squares) and W/Si (dots) multilayers as identified in the inset. The thickness data were obtained from x-ray reflectivity analyses. The multilayers were grown under identical growth conditions. Note that for W/Si the straight lines do not extrapolate to zero at zero growth time.

Fig. 3 Cross-section SEM image of a WSi_2/Si zone-plate multilayer structure. The bright strips are WSi_2, and the dark ones are Si. The substrate is on the left side of the image.

Fig. 4 Measured layer positions from a SEM image for the WSi_2/Si multilayer compared to the targeted layer position.

Fig. 5 Measured inverse layer thicknesses versus layer position compared to the targeted values and the best fit over the 0-8 μm region. The targeted and best fit focal length are 10.89 mm and 10.27 mm at 30 keV, respectively.

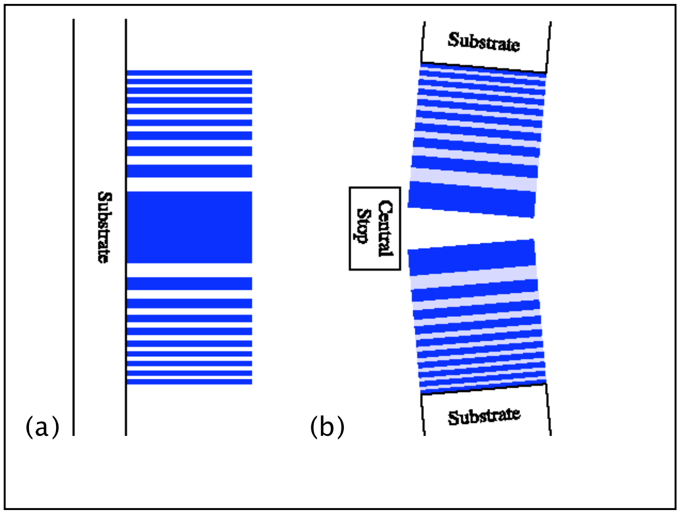

LIU, FIGURE 1

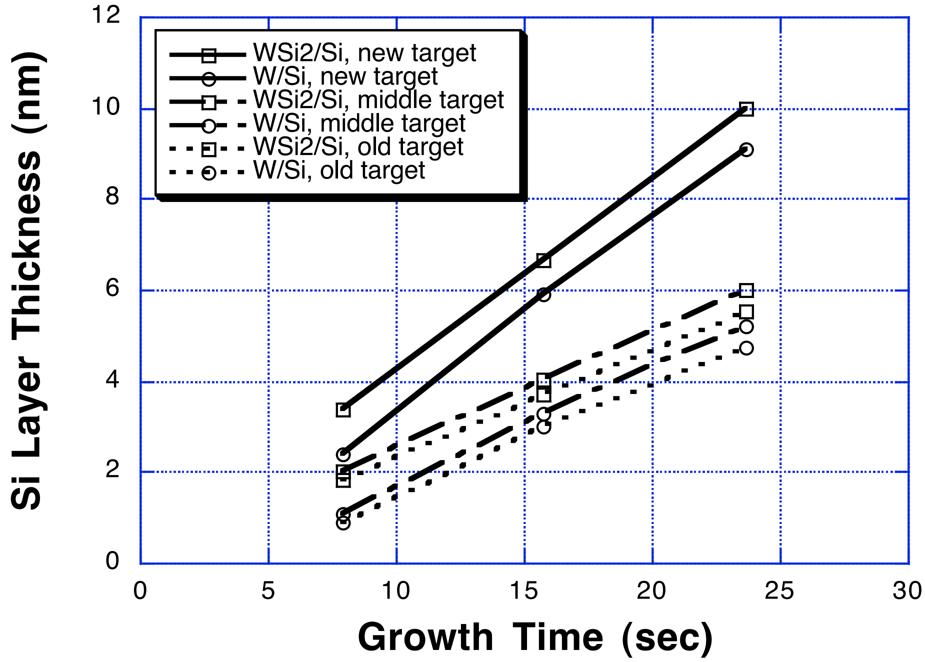

Si Layer Thickness (nm)
Growth Time (sec)
WSi2/Si, new target
W/Si, new target
WSi2/Si, middle target
W/Si, middle target
WSi2/Si, old target
W/Si, old target
0
2
4
6
8
10
12
0
5
10
15
20
25
30

LIU, FIGURE 2

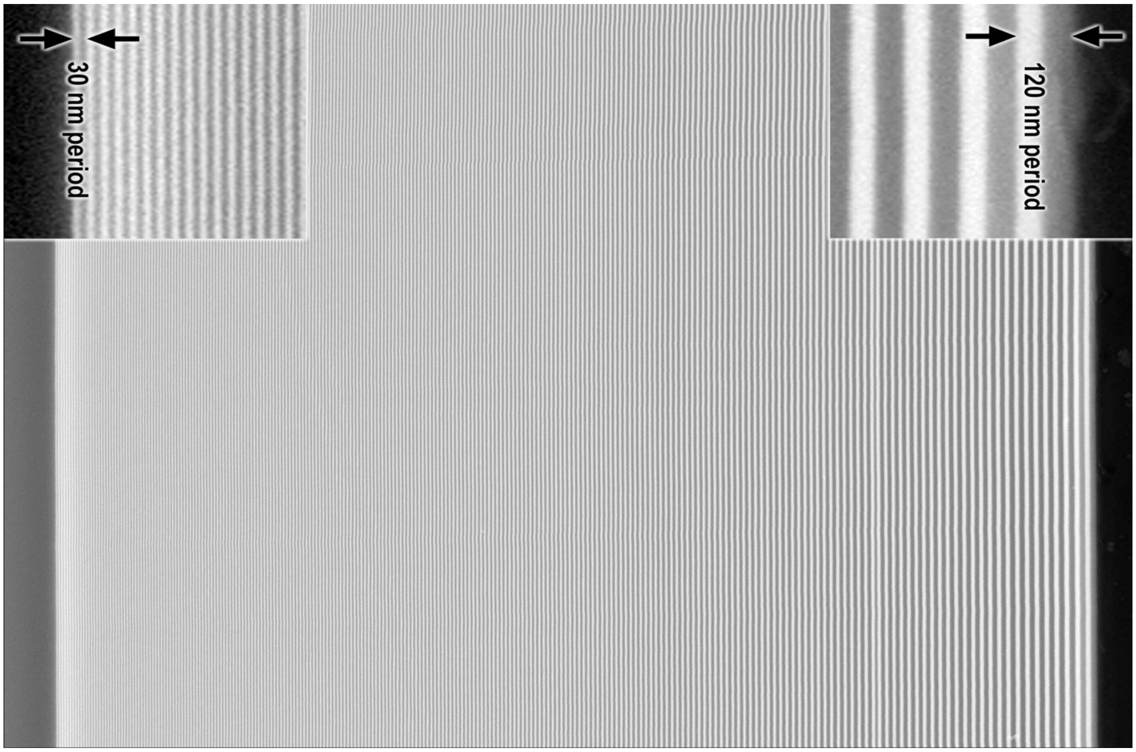

LIU, FIGURE 3

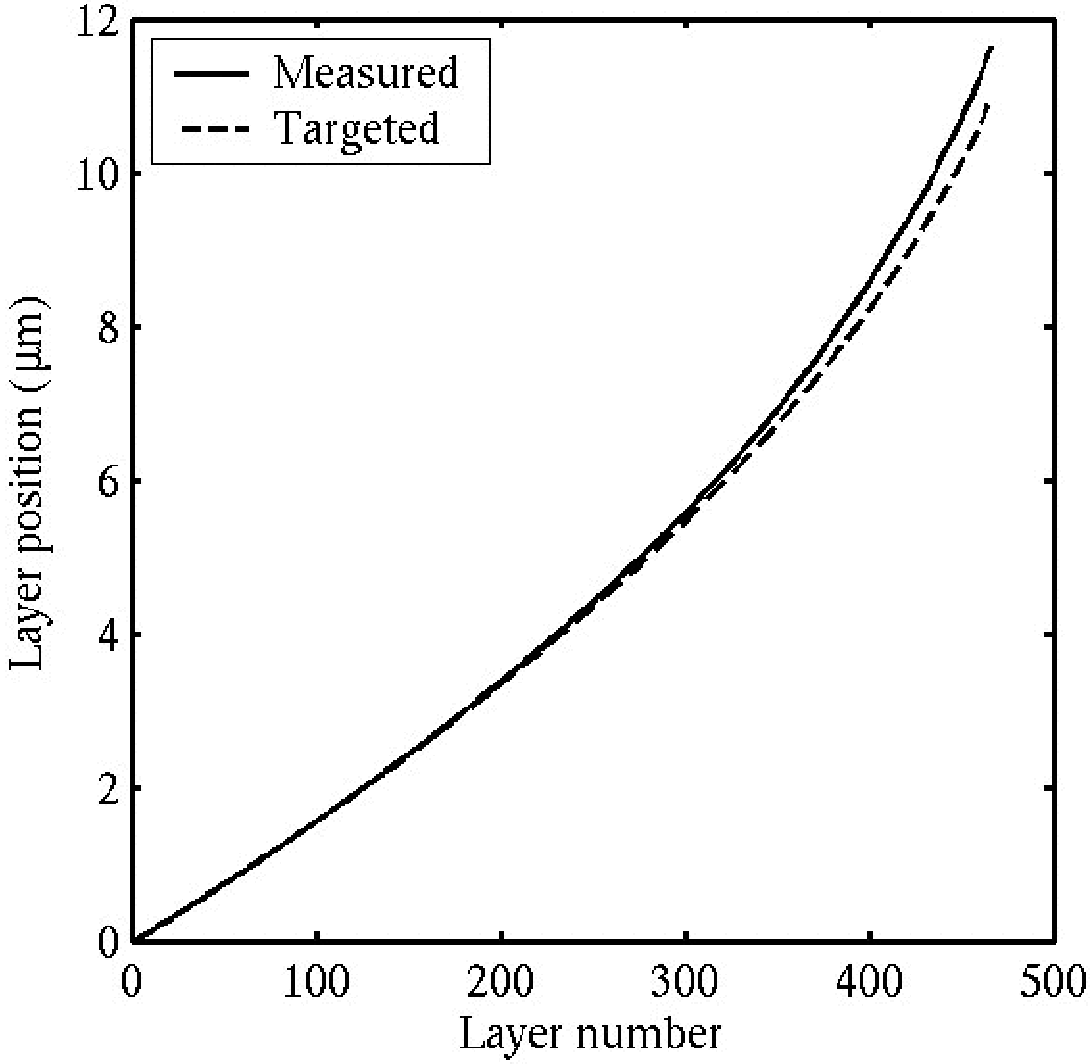

Measured
Targeted
Layer position (µm)
Layer number
0
2
4
6
8
10
12
0
100
200
300
400
500

LIU, FIGURE 4

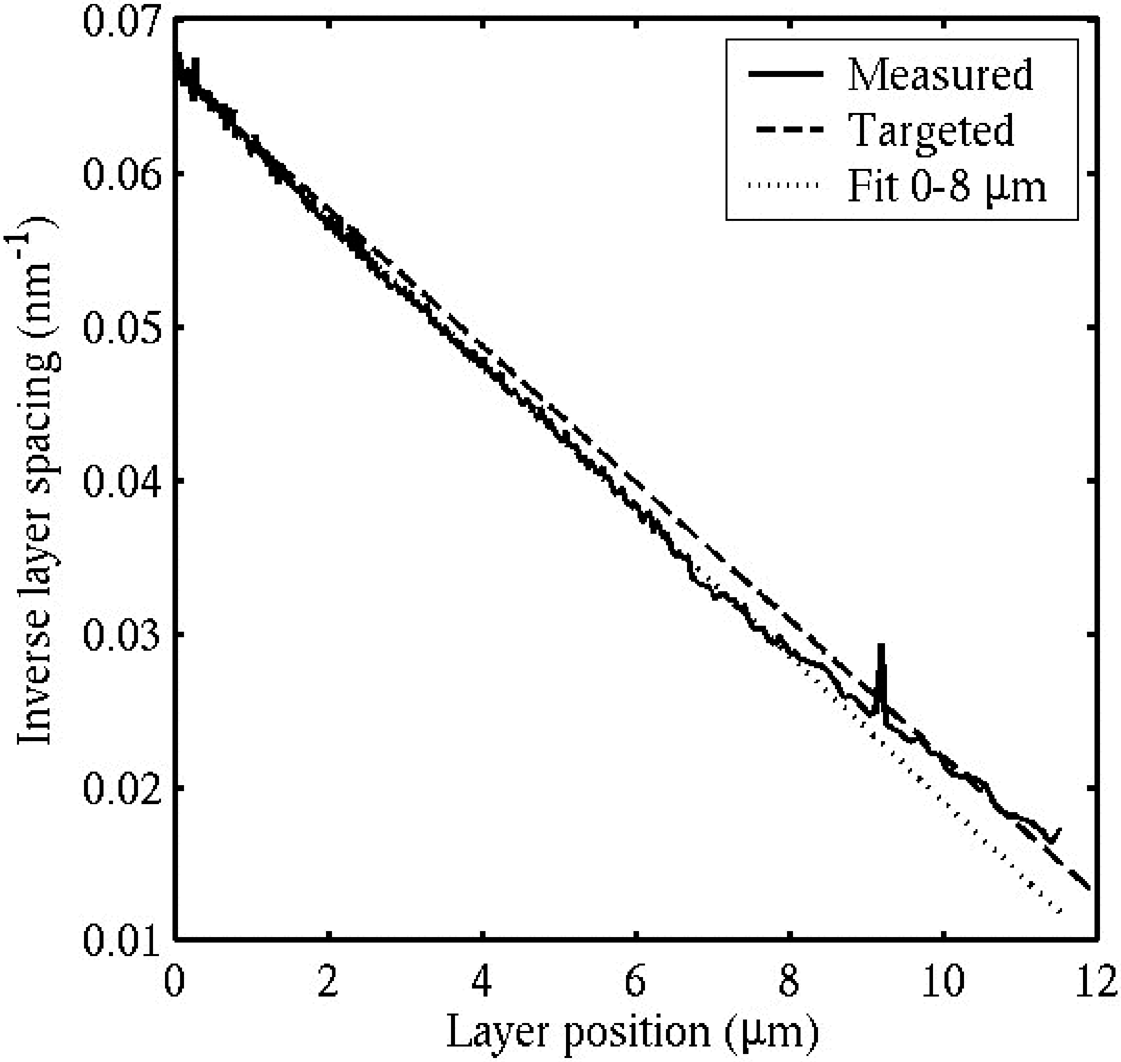

Measured
Targeted
Fit 0-8 µm
Inverse layer spacing (nm^{-1})
Layer position (µm)
0.07
0.06
0.05
0.04
0.03
0.02
0.01
0
2
4
6
8
10
12

LIU, FIGURE 5